ELECTRONIC PROPERTIES
OF SOLID

Electronic Structure of p-Type $La_{1-x}M_x^{2+}MnO_3$ Manganites in the Ferromagnetic and Paramagnetic Phases in the LDA + GTB Approach

V. A. Gavrichkov[a,b], S. G. Ovchinnikov[a,b], I. A. Nekrasov[c], and Z. V. Pchelkina[d]

[a] *Kirensky Institute of Physics, Siberian Branch, Russian Academy of Sciences, Krasnoyarsk, 660036 Russia*
[b] *Siberian Federal University, Krasnoyarsk, 660041 Russia*
[c] *Institute of Electrophysics, Ural Branch, Russian Academy of Sciences, Yekaterinburg, 620016 Russia*
[d] *Institute of Metal Physics, Ural Branch, Russian Academy of Sciences, Yekaterinburg, 620990 Russia*
e-mail: gav@iph.krasn.ru
Received July 16, 2010

Abstract—The band structure, spectral intensity, and position of the Fermi level in doped p-type $La_{1-x}M_x^{2+}MnO_3$ manganites (M = Sr, Ca, Ba) is analyzed using the LDA + GBT method for calculating the electronic structure of systems with strong electron correlations, taking into account antiferro-orbital ordering and using the Kugel–Khomskii ideas and real spin $S = 2$. The results of the ferromagnetic phase reproduce the state of a spin half-metal with 100% spin polarization at $T = 0$, when the spectrum is of the metal type for a quasiparticle with one spin projection and of the dielectric type for the other. It is found that the valence band becomes approximately three times narrower upon a transition to the paramagnetic phase. For the paramagnetic phase, metal properties are observed because the Fermi level is located in the valence band for any nonzero x. The dielectrization effect at the Curie temperature is possible and must be accompanied by filling of d_x orbitals upon doping. The effect itself is associated with strong electron correlations, and a complex structure of the top of the valence band is due to the Jahn–Teller effect in cubic materials.

DOI: 10.1134/S1063776111030101

1. INTRODUCTION

The spin halfmetal (SHM) state of doped manganites was theoretically investigated in [1] and was subsequently confirmed in photoemissive experiments with spin resolution [2]. In experiments [3], the tunnel magnetoresistance at $(LaSr)MnO_3/SrTiO_3/(LaSr)MnO_3$ magnetic tunnel junctions was 1850%, which amounts to 95% when recalculated [4] for spin polarization at $T = 4.2$ K. The SHM state in manganites is also characterized by the simple $1 - \alpha T^{3/2}$ Bloch dependence of the spin polarization (i.e., magnetization of the material). High spin polarization indices make these materials promising for applications at room temperatures. Manganites are crystallized in the simple perovskite structure. It is assumed that prototype compound $LaMnO_3$ is an antiferromagnetic dielectric (charge transfer insulator) in which strong electron correlation (SEC) effects play a significant role. The substitution of bivalent $M^{2+} = Sr^{2+}, Ca^{2+}, Ba^{2+}$ for La^{3+} leads to a metallic ferromagnetic state with a Curie temperature of $T_C \approx 360$ K ($x > 0.2$), above which the material is in the dielectric state. A large number of experimental and theoretical publications are devoted to the metal–insulator transition upon an increase in temperature,

as well as to the colossal magnetoresistance (CMR) effect in the vicinity of T_C in $La_{1-x}M_xMnO_3$ compounds (see, for example, reviews in [5–14]). The double exchange (DE) model [15–17] is an intuitively comprehensible basic model for describing the type of the electronic structure of these materials [7]. However, the DE model cannot quantitatively reproduce the colossal changes in conductivity upon a passage through T_C [18, 19]. The best known solution to the problem was proposed in [20], where it was assumed that magnetic disorder in the PM phase, which leads to a comparatively weak localization of carriers, triggers the formation of localized charge carriers (polarons) due to a strong electron–phonon interaction of the Jahn–Teller type. The result obtained in [20] is in quantitative agreement with the magnitude of the observed effect. However, a group of scientists from Ural [21–23] has not obtained any proofs of the existence of polarons in compounds with CMR at $T > T_C$. Nevertheless, the authors of [24], devoted to analysis of SEC effects in the quasiparticle spectrum, proceeded from the same point of view. According to [24], the Coulomb interaction of e_g electrons facilitates the formation of Jahn–Teller polarons due to increased energy of splitting to $2E_{JT} + U' - J_H$, where (in notation used in [24]) U' is the Coulomb interaction

between the orbitals and J_H is the Hund exchange interaction. We believe that the states with two electrons in the e_g shell are nearly empty both in undoped LaMnO$_3$ materials and in p-type La$_{1-x}$M$_x$MnO$_3$ materials (M = Sr, Ba, Ca). These states form an empty conduction band (analog of the upper Hubbard band) in these materials. Consequently, such effects could be expected only in n-type manganites. The formation of a pseudogap following from numerical calculations based on the dynamic mean field theory (DMFT) probably indicates a charge-nonuniform ground state, which was also studied in [25].

The existence of a pseudogap and its relation to the magnetoresistance in these materials is beyond any doubt [26]; nevertheless, the form of the dependence of the resistance on the field and temperature is still of considerable interest [21−23]. According to the results obtained in [27] on La$_{0.7}$Ca$_{0.3}$MnO$_3$ epitaxial films, the magnetoresistance of manganites exhibits scaling to the dependence of ρ on magnetization M alone: $\rho(T, H) \longrightarrow \rho(M)$ both in the FM and in PM phases; in the latter case, scaling can be traced using the Curie−Weiss susceptibility. The results indicate the existence of a coupling mechanism between the magnetization and conductivity both in the FM and PM regions in these materials.

The goal of this study is to analyze the spectral intensity of the quasiparticle states, density of states, and position of the Fermi level in doped manganites against the background of homogeneous FM and PM states. We use the generalized tight binding (GTB) method developed in [28] for calculating the electronic structure of systems with strong electron correlations (SECs), including manganites [29]. The results of our calculations reproduce the SHM state with complete (100%) spin polarization in the FM phase at $T = 0$ when we have the metal type of the spectrum for a quasiparticle with one spin projection (along the magnetization) and the dielectric type of the spectrum for a quasiparticle of another projection. It is found that the width of the valence band in the PM phase decreases by a factor of $(1/2)\cos(\theta/2) \approx 0.35$ in contrast to its contraction by a factor of $\cos(\theta/2)$ in the double exchange (DE) model, and the origin of quasiparticles themselves changes. In the PM phase, the type of ground state of the material depends on the set of parameters of the Hamiltonian and on the doping level due to orbital ordering and SEC effects.

For ab initio calculation of microscopic parameters in the GTB Hamiltonian for these compounds, we used the LDA + GTB method as it was done in [30] for cuprates. The article is organized as follows. In Section 2, we describe the fundamentals of the LDA + GTB method as applied for calculating the electronic structure of manganites, which differ from cuprates mainly in the high spin of multielectron energy levels and in the perovskite structure. In Section 3, peculiarities and origin of changes in the quasiparticle spec-

trum for doped manganites at the Curie temperature are analyzed on a qualitative, intuitively comprehensible level. The results of numerical calculations for the band structure, spectral intensity of quasiparticle states, density of states, and Fermi level as functions of the hole concentration in the PM and FM phases are considered in Section 4. In Section 5, our conclusions concerning the possibility of interpreting the origin of metal−insulator transition (MIT) in our calculations are formulated.

2. LDA + GTB METHOD AS APPLIED TO MANGANITES

Basic principles for constructing the GTB Hamiltonian and the configuration space for La$_{1-x}$M$_x$MnO$_3$ are described in detail in [29], where we calculated for the first time the dispersion of quasiparticles for this material using the GTB method. However, this approach involves a large number of parameters; for this reason, we develop in this section the LDA + GTB method as it was done in [30] for cuprates. We will mainly consider the physical interpretation of evolution of the quasiparticle spectrum for doped manganites upon a transition from the FM to PM phase, omitting analytic details except those pertaining to new calculations of the spectral intensity of quasiparticle states, density of states, and position of the Fermi level.

As before [29], our calculations will be based on the following initial concepts which are essential, in our opinion, for constructing an adequate theory of the electronic structure in manganites:

(i) allowance for the effects of orbital ordering (cooperative Jahn−Teller effect) [31];

(ii) construction of the configuration space of the electron system based on multielectron states: $d^5p^6(S = 5/2)$, $d^4p^6 + d^5p^5(S = 2)$, and $d^3p^6 + d^4p^5$ ($S = 3/2$);

(iii) allowance for Mn3d−O2p hybridization for a correct description of splitting of the 3d states of manganese in the field of ligands (ligand field splitting [32]).

The cooperative Jahn−Teller effect in manganites leads to the formation of a superlattice $\sqrt{2} \times \sqrt{2}$ in the xy plane. This effect is known as antiferro-orbital ordering [31]. The set of e_g states in LaMnO$_3$ is usually chosen in the form

$$|\theta\rangle = \cos\left(\frac{\theta}{2}\right)|d_{3z^2-r^2}\rangle + \sin\left(\frac{\theta}{2}\right)|d_{x^2-y^2}\rangle,$$

where

$$\left|\theta = \frac{\pi}{3}\right\rangle = \sqrt{3}(y^2 - z^2) \equiv |d_y\rangle,$$

$$\left|\theta = \frac{2\pi}{3}\right\rangle = (3y^2 - r^2) \equiv |d_{3y}\rangle,$$

$$\left|\theta = \frac{4\pi}{3}\right\rangle = (3x^2 - r^2) \equiv |d_{3x}\rangle, \qquad (1)$$

$$\left|\theta = \frac{5\pi}{3}\right\rangle = \sqrt{3}(x^2 - z^2) \equiv |d_x\rangle.$$

Accordingly, the division of $2p$ oxygen orbitals forming σ bonds into sublattices is carried out as follows: two p_x orbitals (p_{1x} and p_{2x}) and one p_z orbital in the A sublattice, and two p_y orbitals (p_{1y} and p_{2y}) and one p_z orbital in the B sublattice. Half-filled t_{2g} states form a rigid spin $S = 3/2$, which will be subsequently used for constructing multielectron states of the configuration space of the problem [29].

Let us confine our analysis to a simple cubic structure with Jahn–Teller distortions [29]. Therefore, we have a simple cubic Brillouin zone in our calculation, and allowance for distortions lowers the symmetry to tetragonal. In fact, manganites have a more complex P_{nma} structure that can be formed from the cubic structure not only due to cooperative distortion of octahedrons ($\sqrt{2} \times \sqrt{2}$ superlattice), but also by their rotation relative to one another. For the unit cell, we choose a distorted MnO_6 octahedron. The states of La^{2+} and the bivalent ion $M^{2+} = Sr^{2+}, Ca^{2+}, Ba^{2+}$ substituting it are disregarded in calculations; we assume that these states ensure electroneutrality (i.e., we have a reservoir whose charge depends on x). The Hamiltonian of the electron pd subsystem can be written in the form

$$\hat{H} = \hat{H}_d + \hat{H}_p + \hat{H}_{pp} + \hat{H}_{pd},$$

$$\hat{H}_d = \sum_{i\lambda\sigma}\left[(\varepsilon_\lambda - \mu)\hat{d}^+_{\lambda i\sigma}\hat{d}_{\lambda i\sigma} + \frac{1}{2}U_\lambda \hat{n}^\sigma_{\lambda i}\hat{n}^{-\sigma}_{\lambda i}\right.$$

$$\left. + \sum_{\lambda'\sigma'}(-J_d\hat{d}^+_{\lambda i\sigma}\hat{d}_{\lambda i\sigma'}\hat{d}^+_{\lambda' i\sigma'}\hat{d}_{\lambda' i\sigma} + V_{\lambda\lambda'}\hat{n}^\sigma_{\lambda i}\hat{n}^{\sigma'}_{\lambda' i})\right],$$

$$\hat{H}_p = \sum_{r\alpha\sigma}\left[(\varepsilon_\alpha - \mu)\hat{p}^+_{\alpha r\sigma}\hat{p}_{\alpha r\sigma} + \frac{1}{2}U_\alpha \hat{n}^\sigma_{\alpha r}\hat{n}^{-\sigma}_{\alpha r}\right.$$

$$\left. + \sum_{\alpha'\sigma'}\left(-J_p\hat{p}^+_{\alpha r\sigma}\hat{p}_{\alpha r\sigma'}\hat{p}^+_{\alpha' r\sigma'}\hat{p}_{\alpha' r\sigma} + V_{\alpha\alpha'}\hat{n}^\sigma_{\alpha r}\hat{n}^{\sigma'}_{\alpha' r}\right)\right], \qquad (2)$$

$$\hat{H}_{pd} = \sum_{\langle ir\rangle}\sum_{\alpha\lambda\sigma\sigma'}[(t_{\lambda\alpha}\hat{p}^+_{\alpha r\sigma}\hat{d}_{\lambda i\sigma} + \text{H.c.} + V_{\alpha\lambda}\hat{n}^\sigma_{\alpha r}\hat{n}^{\sigma'}_{\lambda i})$$

$$- J_{pd}(\hat{d}^+_{\lambda i\sigma}\hat{d}_{\lambda i\sigma}\hat{p}^+_{\alpha r\sigma}\hat{p}_{\alpha r\sigma} + \text{H.c.})],$$

$$\hat{H}_{pp} = \sum_{\langle rr'\rangle}\sum_{\alpha\beta\sigma}(t_{\alpha\beta}\hat{p}^+_{\alpha r\sigma}\hat{p}_{\beta r\sigma} + \text{H.c.}),$$

where $\hat{n}^\sigma_{\lambda i} = \hat{d}^+_{\lambda i\sigma}\hat{d}_{\lambda i\sigma}$ and $\hat{n}^\sigma_{\alpha r} = \hat{p}^+_{\alpha r\sigma}\hat{p}_{\alpha r\sigma}$. Indices $\mathbf{i}$ and $\mathbf{r}$ run through positions $d_x, d_{3y}, p_{x_1}, p_{x_2},$ and p_z in the A sublattice and $d_y, d_{3x}, p_{y_1}, p_{y_2},$ and p_z in the B sublattice of localized atomic orbitals, respectively. Analogously, $\varepsilon_\lambda = \varepsilon_{d_x}$ ($\lambda = d_x, d_{3x}, d_y, d_{3y}$) and $\varepsilon_\alpha = \varepsilon_p$ ($\alpha = p_x, p_y, p_z$) are the energies of the atomic orbitals of $3d$ manganese and $2p$ oxygen, respectively. The matrix elements of the manganese–oxygen hopping are t_{pd} for $\lambda = d_x, d_y$; $\alpha = p_x, p_y, p_z$ and $2t_{pd}/\sqrt{3}$ for $\lambda = d_{3x}, d_{3y}, \alpha = p_x, p_y$ of the hopping t_{pp} between nearest oxygen ions;

$$U_\lambda = \begin{cases} U_d, & \lambda = \lambda' \\ V_{dd}, & \lambda \neq \lambda' \end{cases} \quad (\lambda = d_x, d_y, d_{3x}, d_{3y})$$
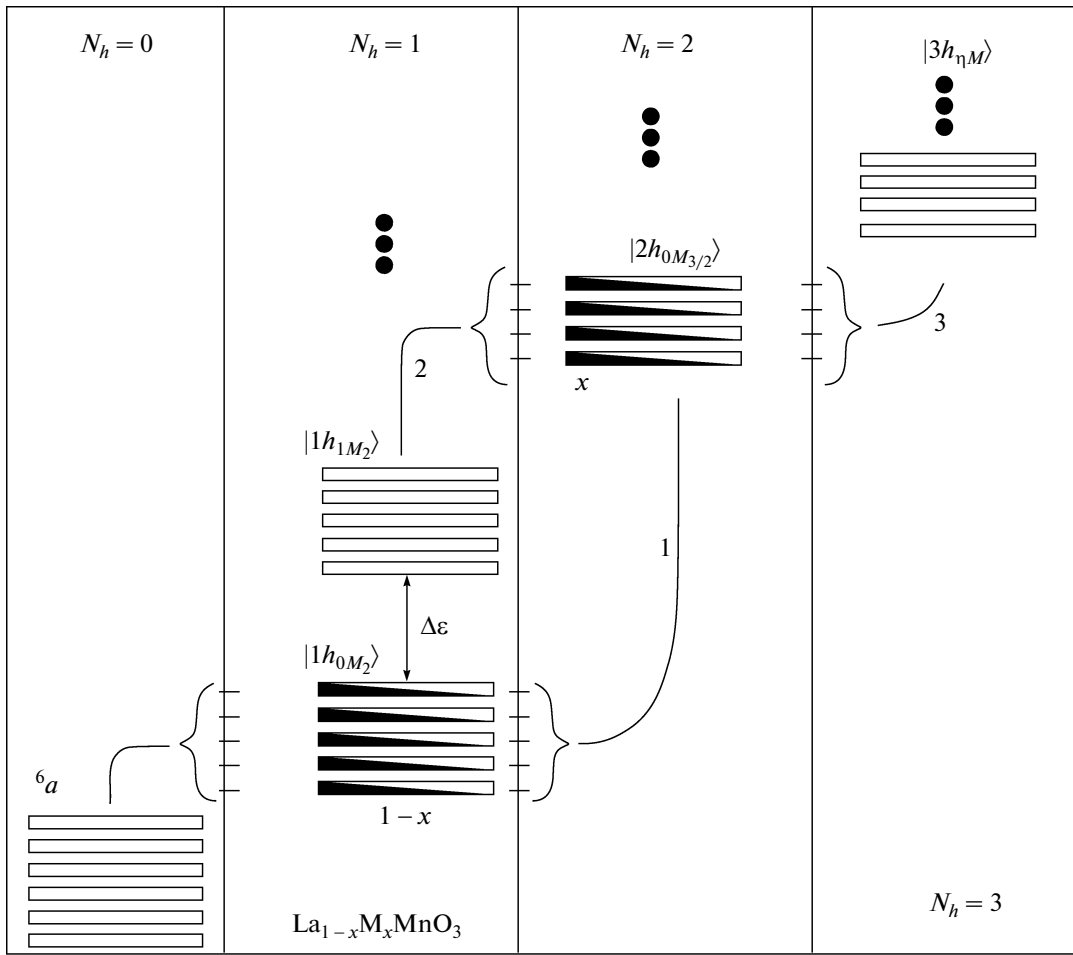
and

$$U_d = \begin{cases} U_p, & \alpha = \alpha' \\ V_{pp}, & \alpha \neq \alpha' \end{cases} \quad (\alpha = p_x, p_y, p_z)$$

are intraatomic Coulomb interactions. $V_{\alpha\lambda} = V_{pd}$ are the energies of Coulomb repulsion between manganese and oxygen; and J_d, J_p, and J_{pd} describe the exchange interaction in manganese, oxygen, and Mn–O. Henceforth, we will assume for simplicity that all matrix elements of the Coulomb interaction are independent of the form of d or p orbitals (i.e., $U_d = V_{dd}$ and $U_p = V_{pp}$).

In determining the parameters of the GTB Hamiltonian, we performed the LDA calculations proceeding from the actual structure P_{nma} of the material. The difficulties encountered in these calculations were associated with the difference between P_{nma} and the cubic structure with orbital ordering. Indeed, in the actual structure of manganites, not only the local distortion effects are observed in oxygen octahedrons and their assembly into a relevant structural motif. The actual structure is attained upon rotation of octahedrons about one or several axes of the initial cubic structure in view of the mismatch between the volume of the La ion and the volume of the dodecahedron between oxygen octahedrons, whose measure is the deviation of the tolerance factor [33] from unity (smaller than 1).

The parameters for our calculations were obtained by simple averaging over rotations of oxygen octahedrons. We give here the values of local energies of electrons and hopping matrix elements (in electronvolts), which have already been averaged and will be used in our subsequent calculations of the quasiparticle spectrum of manganites irrespective of their doping level (eV):

$$\varepsilon_d = \varepsilon_{d_{3x}} = \varepsilon_{d_y} = -0.28,$$

$$\varepsilon_p = \varepsilon_{p_y} = \varepsilon_{p_z} = -3.76,$$

$$\varepsilon_{p_x} = -3.52, \quad t_{pd} = t_{p_z d_y} = t_{p_y d_y} = 1.41,$$

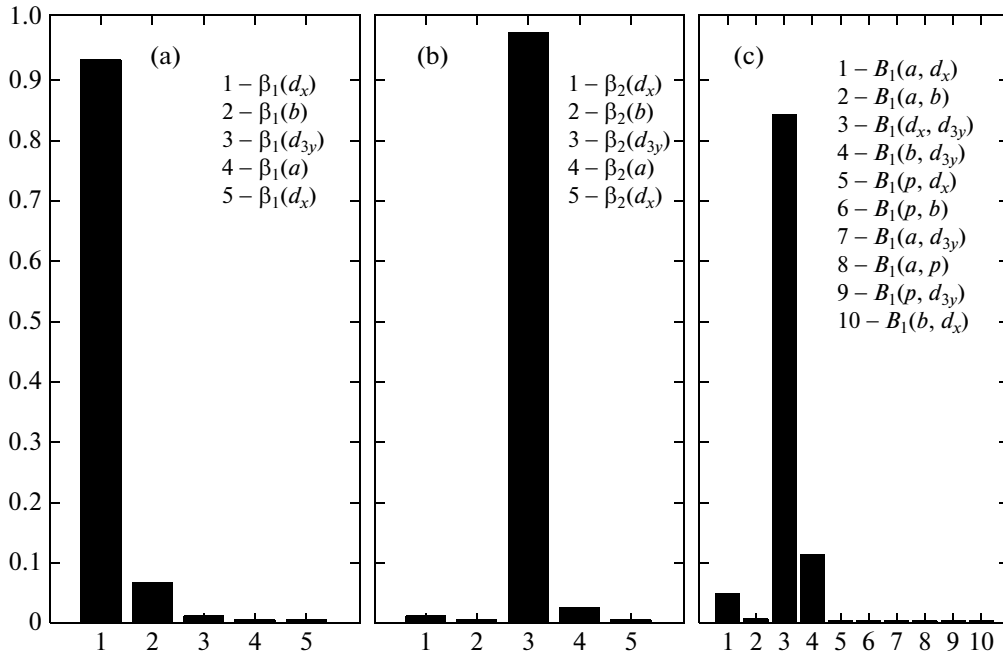$$t'_{pd} = t_{p_x d_{3x}} = 2.0, \quad t'_{pp} = t_{p_x p_y} = t_{p_x p_z} = 0.52, \qquad (3)$$

Fig. 1. Multielectron basis for various sectors of the Hilbert space, which are characterized by number of holes N_h in the MnO_6 cluster. The "vacuum" state $N_h = 0$ corresponds to the d^5p^6 configuration. Spin sublevels are shown for each multiplet. One-electron excitations (Fermi quasiparticles) are depicted by solid curves as transitions between $(pd)^{n+1}$ and $(pd)^n$ terms. The diagram of formation of quasiparticle excitations with a nonzero spectral intensity in the PM phase: quasiparticles 1 form the top of the valence band; quasiparticles 2 describe in-gap states, their spectral intensity is proportional to doping level x; quasiparticles 3 form the complete packet of valence bands, their spectral intensity is proportional to doping level x.

$$t_{pp} = t_{p_xp_y} = 0.47, \quad U_p = V_p = 4, \quad U_d = V_d = 8,$$

$$J_d = 1.5, \quad V_{pd} = 2, \quad J_{pd} = J_{pp} = 0.$$

The notation for the parameters corresponds to the B octahedron in Fig. 1 in [29]. The corresponding parameters for octahedron A can be obtained by substitution $x \longleftrightarrow y$. According to the results of LDA calculations, d_x and d_{3y} in a less symmetric actual structure are mixed even in the unit cell. However, mixing effects disappear together with the rotation of octahedrons. In our analysis, we followed the LDA + GTB algorithm [30], in which the Hamiltonian with calculated parameters is transformed to a symmetric unit cell basis (with the cell centered at the manganese ion) consisting of d_y, d_{3x}, and d_x, d_{3y} basis, as well as unit cell group oxygen orbitals $|a\rangle$, $|b\rangle$, and $|p\rangle$ instead of the initial atomic p orbitals of oxygen [29]. These group orbitals are orthogonal at neighboring cells. Further, the Hamiltonian is divided into two parts

containing intra- and intercell interactions ($\hat{H} = \hat{H}_0 + \hat{H}_{cc}$). After exact diagonalization of the one cell part of the Hamiltonian side, all intercell interactions $\hat{H}_{cc}$ are written in the representation of eigenstates of $\hat{H}_0$, which have already been calculated. Depending in the required accuracy in final results, various approximations are used for $\hat{H}_{cc}$. Here, we are using the Hubbard I approximation, which in the two-sublattice case leads to results close to those obtained using the quantum-mechanical Monte Carlo method.

To explain the electronic structure using the multielectron approach, we must consider the results of exact diagonalization intracell Hamiltonian $\hat{H}_0$ in greater detail. The results of exact diagonalization are shown schematically in Fig. 1, in which various sectors of the configuration space are presented. The main

Fig. 2. Squares of the expansion coefficients for wavefunction of (a) ground state $|1h_{0M_2}\rangle$; (b) first excited state $|1h_{1M_2}\rangle$ on the one-particle sector, and (c) ground state $|2h_{0M_{3/2}}\rangle$ in the two-particle sector in initial functions $|h_\lambda, M_2\rangle$ and $|h_\lambda, h_{\lambda'}, M_{3/2}\rangle$.

sector is $d^4p^6 + d^5p^5$ ($S = 2$, spin projection M_2) with a single hole per unit cell ($N_h = 1$) because the state with the lowest energy in this sector is completely filled in the initial $LaMnO_3$ structure.

In accordance with the number of possible arrangements of the hole at five initial states ($|h_a, M_S\rangle$, $|h_{d_{3y}}, M_S\rangle$, and $|h_{d_x}, M_S\rangle$, $|h_b, M_S\rangle$, $|h_p, M_S\rangle$), we have five spin multiplets $|1h_{\mu M_S}\rangle = \sum_\lambda \beta_\mu(h_\lambda)|h_\lambda, M_S\rangle$, where $S = 2$, $\lambda = a, d_{3y}, b, p, d_x$ and $\mu = 0$ to 4 with energies $\varepsilon_{\mu M_2}$ determined in the course of exact diagonalization, as well as three spin multiplets with spin $S = 3$. Jahn–Teller distortions in the oxygen octahedron lead to splitting of the orbital ^5e_g doublet, and we have two orbital-nondegenerate states in the one-hole sector. Depending on the parameters, the splitting between the ground state $|1h_{0M_2}\rangle$ and first excited state $|1h_{1M_2}\rangle$ is on the order of $\Delta\varepsilon \approx 0.2$–$0.5$ eV (Fig. 1). The prevailing d_x and d_{3y} nature of the ground state and the first excited state follows from calculation of weights $\beta_\mu^2(h_\lambda)$ in Figs. 2a and 2b.

In the two-hole sector $d^3p^6 + d^4p^5 + d^5p^4$, the situation with ten spin ($S = 3/2$) multiplets $|2h_{\tau M_{3/2}}\rangle = \sum_{\lambda\lambda'} B_\tau(h_\lambda, h_{\lambda'})|h_\lambda, h_{\lambda'} M_{3/2}\rangle$, $\tau = 0$ to 9, is observed, in which energies $\varepsilon_{\tau M_{3/2}}$ are characterized by an isolated

ground state $|2h_{0M_{3/2}}\rangle$ separated from the excited states by an interval of at least 1 eV, as well as nine high-spin ($S = 5/2$) multiplets (two e_g holes make zero contribution). The results of calculation of weights $B_\tau^2(h_\lambda, h_{\lambda'})$ in Fig. 2c show that in spite of pd hybridization, ground state $|2h_{\tau = 0, M_{3/2}}\rangle$ is also of predominantly $d_x d_{3y}$ type.

For our further analysis of the intercell part $\hat{H}_{cc}$ of the Hamiltonian, we will use the representation of Hubbard operators $\hat{X}_f^{pq} = |p\rangle\langle q|$ [34] acting in the space of multielectron eigenstates $|p\rangle$ ($|q\rangle$) for $\hat{H}_0$. We can write all one-electron operators with the help of Hubbard operators $\hat{c}_{\lambda f\sigma} = \sum_m \gamma_{\lambda\sigma}(m)\hat{X}_f^m$, where $\hat{c}_{\lambda f\sigma} = \hat{d}_{xf\sigma}, \hat{d}_{3yf\sigma}, \hat{a}_{f\sigma}, \hat{b}_{f\sigma}, \hat{p}_{zf\sigma}$, with the introduction of the system of root vectors $\boldsymbol{\alpha}_m$ in accordance with the scheme

$$\hat{X}_f^{pq} \longrightarrow \hat{X}_f^{\boldsymbol{\alpha}_m} \longrightarrow \hat{X}_f^m.$$

The matrix elements of the hopping amplitude $\gamma_{\lambda\sigma}(m) = \langle p|\hat{c}_{\lambda f\sigma}|q\rangle$ can be calculated directly using coefficients $B_\tau(h_\lambda, h_{\lambda'})$ and $\beta_\mu(h_\lambda)$ and are partial amplitudes of transitions between individual multielectron states. Following this scheme, we can write the Hamiltonians for hopping in the orbital-ordered two-sublattice representation in the form

$$H_{cc} = \sum_{\lambda\lambda'\sigma}\sum_{mn}\{\gamma_{\lambda\sigma}^*(m)\gamma_{\lambda'\sigma}(n)$$

$$\times [\,T_{\lambda\lambda'}(\mathbf{R}_{AA})\hat{X}_{f_A}^{+m}\hat{X}_{f_A+\mathbf{R}_{AA}}^{-n}$$

$$+ T_{\lambda\lambda'}(\mathbf{R}_{BB})\hat{Y}_{f_B}^{+m}\hat{Y}_{f_B+\mathbf{R}_{BB}}^{-n} \qquad (4)$$

$$+ T_{\lambda\lambda'}(\mathbf{R}_{AB})\hat{X}_{f_A}^{+m}\hat{Y}_{f_A+\mathbf{R}_{AB}}^{-n}$$

$$+ T_{\lambda\lambda'}(\mathbf{R}_{BA})\hat{Y}_{f_B}^{+m}\hat{X}_{f_B+\mathbf{R}_{BA}}^{-n}] + \text{H.c.}\,\}.$$

Further, using the system of equations for operators $\hat{X}_{f_A}^m$ and $\hat{Y}_{f_B}^n$ for both A and B sublattices, we obtain

$$i\dot{\hat{X}}_{f_A}^m = [\hat{X}_{f_A}^m, \hat{H}] = \Omega_m\hat{X}_{f_A}^m + [\hat{X}_{f_A}^m, \hat{H}_{cc}]$$

$$= \Omega_m\hat{X}_{f_A}^m + \sum_{\lambda\lambda's}\sum_{pq}\sum_{i_A}\Big\{\sum_{\mathbf{R}_{AA}}T_{\lambda\lambda'}(\mathbf{R}_{AA})$$

$$\times \{\gamma_{\lambda s}^*(p)\gamma_{\lambda's}(q)[X_{f_A}^m, X_{i_A}^{+p}X_{i_A+\mathbf{R}_{AA}}^q]$$

$$+ \gamma_{\lambda's}^*(q)\gamma_{\lambda s}(p)[X_{f_A}^m, X_{i_A+\mathbf{R}_{AA}}^{+q}X_i^p]\,\}$$

$$+ \sum_{\mathbf{R}_{AB}}T_{\lambda\lambda'}(\mathbf{R}_{AB})\{\gamma_{\lambda s}^*(p)\gamma_{\lambda's}(q)[X_{f_A}^m, X_{i_A}^{+p}Y_{i_A+\mathbf{R}_{AB}}^q]$$

$$+ \gamma_{\lambda's}^*(q)\gamma_{\lambda s}(p)[X_{f_A}^m, Y_{i_A+\mathbf{R}_{AB}}^{+q}X_{i_A}^p]\,\}$$

$$+ \sum_{\mathbf{R}_{BA}}T_{\lambda\lambda'}(\mathbf{R}_{BA})\{\gamma_{\lambda s}^*(p)\gamma_{\lambda's}(q)[X_{f_A}^m, Y_i^{+p}Y_{i_B+\mathbf{R}_{BA}}^q] \qquad (5)$$

$$+ \gamma_{\lambda's}^*(q)\gamma_{\lambda s}(p)[X_{f_A}^m, Y_{i+\mathbf{R}_{BA}}^{+q}Y_{i_B}^p]\,\}\Big\} \approx \Omega_m\hat{X}_{f_A}^m$$

$$+ \sum_{\lambda\lambda's}\sum_n\Big\{\sum_{\mathbf{R}_{AA}}T_{\lambda\lambda'}(\mathbf{R}_{AA})$$

$$\times F_{f_A}(m)\{\gamma_{\lambda s}^*(m)\gamma_{\lambda's}(n)X_{f_A+\mathbf{R}_A}^n$$

$$+ \gamma_{\lambda's}^*(m)\gamma_{\lambda s}(n)X_{f_A-\mathbf{R}_A}^n\}$$

$$+ \sum_{\mathbf{R}_{AB}}F_{f_A}(m)T_{\lambda\lambda'}(\mathbf{R}_{AB})\gamma_{\lambda s}^*(m)\gamma_{\lambda's}(n)Y_{f_A+\mathbf{R}_{AB}}^n$$

$$+ \sum_{\mathbf{R}_{BA}}T_{\lambda\lambda'}(\mathbf{R}_{BA})\gamma_{\lambda's}^*(m)\gamma_{\lambda s}(n)Y_{f_A-\mathbf{R}_{BA}}^n\Big\},$$

where $\Omega_m^G = \Omega^G(\alpha_m) = \varepsilon_q^G - \varepsilon_p^G$ is the local energy of quasiparticles, and occupation factor $F_G(m) = \langle X_{f_G}^{pp}\rangle + \langle X_{f_G}^{qq}\rangle$ determines the spectral intensity of quasiparticle states (analogously, for $\hat{Y}_{f_B}^n$ with substitution $X \longleftrightarrow$

Y and $A \longleftrightarrow B$). Let us introduce Green's functions on operators $\hat{X}_{i_A}^m$ and $\hat{Y}_{i_B}^n$:

$$\hat{D}_{ij} = \begin{pmatrix} \hat{D}_{i_A j_A} & \hat{D}_{i_A j_B} \\ \hat{D}_{i_B j_A} & \hat{D}_{i_B j_B} \end{pmatrix}, \qquad (6)$$

$$D_{i_A j_B}^{mn} = \langle\langle\hat{X}_{i_A}^m|\hat{Y}_{i_B}^n\rangle\rangle_{E+i0}.$$

Here, the elements of the matrix Green function can be determined from the equations

$$(E - \Omega_m)D_{i_A j_A}^{mn} = \delta_{mn}\delta_{i_A j_A}F_{i_A}(m)$$

$$+ \sum_{\lambda\lambda's p}\sum_{\mathbf{R}_{AA}}F_{i_A}(m)T_{\lambda\lambda'}(\mathbf{R}_{AA}) \qquad (7)$$

$$\times \{\gamma_{\lambda s}^*(m)\gamma_{\lambda's}(p)D_{i_A+\mathbf{R}_{AA}, j_A}^{pn}$$

$$+ \gamma_{\lambda's}^*(m)\gamma_{\lambda s}(p)D_{i_A-\mathbf{R}_{AA}, j_A}^{pn}\} + \sum_{\mathbf{R}_{AB}}F_{i_A}(m)$$

$$\times \{T_{\lambda\lambda'}(\mathbf{R}_{AB})\gamma_{\lambda s}^*(m)\gamma_{\lambda's}(p)D_{i_A+\mathbf{R}_{AB}, j_A}^{pn}$$

$$+ T_{\lambda\lambda'}(\mathbf{R}_{BA})\gamma_{\lambda s}^*(m)\gamma_{\lambda s}(p)D_{i_A-\mathbf{R}_{BA}, j_A}^{pn}\}.$$

Analogously, we write the equations for $D_{i_B j_B}^{mn}(BB)$ for the B sublattice. Having defined the Fourier transform of Green's functions as

$$D_{i_A j_B}^{mn} = \frac{2}{N}\sum_{\mathbf{k}}D_{\mathbf{k}}^{mn}(AB)e^{i\mathbf{k}\cdot\mathbf{R}_{AB}},$$

we obtain

$$D_{\mathbf{k}}^{mn}(AA) = \delta_{mn}\delta_{ij}D_m^{(0)}(AA) + D_m^{(0)}(AA)$$

$$\times \sum_{\lambda\lambda's}\sum_p T_{\lambda\lambda'}^{AA}(\mathbf{k})\{\gamma_{\lambda s}^*(m)\gamma_{\lambda's}(p) + \gamma_{\lambda's}^*(m)\gamma_{\lambda s}(p)\}$$

$$\times D_{\mathbf{k}}^{pn}(AA) + D_m^{(0)}(AA)$$

$$\times \sum_{\lambda\lambda's}\sum_p \{T_{\lambda\lambda'}^{AB}(\mathbf{k})\gamma_{\lambda s}^*(m)\gamma_{\lambda's}(p) \qquad (8)$$

$$+ T_{\lambda\lambda'}^{BA}(\mathbf{k})\gamma_{\lambda s}^*(m)\gamma_{\lambda s}(p)\}D_{\mathbf{k}}^{pn}(BA);$$

$$T_{\lambda\lambda'}^{AB}(\mathbf{k}) = \frac{2}{N}\sum_{\mathbf{R}_{AB}}T_{\lambda\lambda'}^{mn}(\mathbf{R}_{AB})e^{i\mathbf{k}\cdot\mathbf{R}_{AB}}$$

$$= \frac{2}{N}\sum_{\mathbf{R}_{AB}}T_{\lambda\lambda'}^{mn}(-\mathbf{R}_{AB})e^{-i\mathbf{k}\cdot\mathbf{R}_{AB}},$$

$$D_m^0(AA) = \frac{F_A(m)}{E - \Omega_m^A + i0},$$

where $D_m^0(AA)$ is the Green function in the zeroth approximation. The equations of motion for function $D_{i_A j_B}^{mn}$, which are constructed on the operators from different sublattices, have the form

$$D_{\mathbf{k}}^{mn}(AB) = D_m^{(0)}(AA)\sum_{\lambda\lambda's}\sum_p T_{\lambda\lambda'}^{AA}(\mathbf{k})$$

$$\times \{\gamma_{\lambda s}^*(m)\gamma_{\lambda' s}(p) + \gamma_{\lambda's}^*(m)\gamma_{\lambda s}(p)\}D_{\mathbf{k}}^{pn}(AB)$$

$$+ D_m^{(0)}(AA)\sum_{\lambda\lambda's}\sum_p \{T_{\lambda\lambda'}^{AB}(\mathbf{k})\gamma_{\lambda s}^*(m)\gamma_{\lambda's}(p) \tag{9}$$

$$+ T_{\lambda\lambda'}^{BA}(\mathbf{k})\gamma_{\lambda's}^*(m)\gamma_{\lambda s}(p)\}D_{\mathbf{k}}^{pn}(BB).$$

Analogously, we write the equations for $D_{\mathbf{k}}^{mn}(BA)$ with the substitution $A \longleftrightarrow B$. Introducing the notation for the effective hopping,

$$T_{\mathrm{eff},mn}^{AB}(\mathbf{k}) = \sum_{\lambda\lambda'}\sum_\sigma [T_{\lambda\lambda'}^{AB}(\mathbf{k})\gamma_{\lambda\sigma}^*(m)\gamma_{\lambda'\sigma}(n)$$

$$+ T_{\lambda\lambda'}^{BA}(\mathbf{k})\gamma_{\lambda'\sigma}^*(m)\gamma_{\lambda\sigma}(n)], \tag{10}$$

we can use the matrix notation for the resultant system of equations,

$$\hat{D}_{\mathbf{k}} = \hat{\Pi}^{-1}(\mathbf{k})\hat{D}^{(0)}, \tag{11}$$

where

$$\hat{\Pi}(\mathbf{k}) = \begin{pmatrix} 1 - \hat{D}^{(0)}(AA)2\hat{T}_{\mathrm{eff}}^{AA}(\mathbf{k}) & -\hat{D}^{(0)}(AA)2\hat{T}_{\mathrm{eff}}^{AB}(\mathbf{k}) \\ -\hat{D}^{(0)}(BB)2\hat{T}_{\mathrm{eff}}^{BA}(\mathbf{k}) & 1 - \hat{D}^{(0)}(BB)2\hat{T}_{\mathrm{eff}}^{BB}(\mathbf{k}) \end{pmatrix},$$

$$\hat{D}^{(0)} = \begin{pmatrix} \hat{\boldsymbol{D}}^{(0)}(AA) & 0 \\ 0 & \hat{D}^{(0)}(BB) \end{pmatrix}. \tag{12}$$

Thus, the dispersion relations for quasiparticles are defined by the following equation for the poles of matrix Green function $\hat{D}_{\mathbf{k}}$:

$$\left\| \begin{matrix} (E - \Omega_m^A)\delta_{mn} - F_A(m)T_{\mathrm{eff},mn}^{AA}(\mathbf{k}) & -T_{\mathrm{eff},mn}^{AB}(\mathbf{k}) \\ -T_{\mathrm{eff},mn}^{BA}(\mathbf{k}) & (E - \Omega_m^B)\delta_{mn} - F_B(m)T_{\mathrm{eff},mn}^{BB}(\mathbf{k}) \end{matrix} \right\| = 0, \tag{13}$$

whose specific features are reflected in the hopping matrix $T_{\mathrm{eff},mn}^{AB}(\mathbf{k})$, local energies Ω_m for excitations $(pd)^n \longleftrightarrow (pd)^{n\pm1}$, and the set of root vectors $\boldsymbol{\alpha}_m$.

In the general case, to determine the contributions from electron transitions with $\sigma = \pm1/2$ to the formation of a quasiparticles with a certain $\boldsymbol{\alpha}_m$, we must calculate its spectral intensity,

$$A_\sigma(\mathbf{k}, E) = \left(-\frac{1}{\pi}\right)\sum_\lambda \mathrm{Im}(G_{\mathbf{k}\sigma}^{\lambda\lambda})$$

$$= \left(-\frac{1}{\pi}\right)\sum_{\lambda mn}\gamma_{\lambda\sigma}(m)\gamma_{\lambda\sigma}^*(n) \tag{14}$$

$$\times \mathrm{Im}\{D_{\mathbf{k}}^{mn}(AA) + D_{\mathbf{k}}^{mn}(BB)\}_{E+i0},$$

where $G_{\mathbf{k}\sigma}^{\lambda\lambda} = \langle\langle c_{\mathbf{k}\lambda\sigma}|c_{\mathbf{k}\lambda\sigma}^+\rangle\rangle_{E+i0}$. The spectral intensity for some types of quasiparticles turns out to be negligibly low or even zero due to the occupation factor (the initial and final states are unoccupied). Consequently, the corresponding quasiparticle peak is simply not there. Numerical calculation of the spectral intensity based on formula (14) was performed along symmetric

directions of the Brillouin zone at $T = 0$ in the FM and PM phases. Owing to the SEC effects, the spectral intensity can be redistributed [35] among the subbands, which are of Jahn–Teller origin in the given case. As a result, the partial number of states in the valence band depends on concentration x of the dopant component M^{2+}.

3. PECULIARITIES OF THE ELECTRON SPECTRUM OF MANGANITES IN THE PM AND FM STATES

The origin of quasiparticles defined by Eqs. (13) and (14) can be clarified by the following qualitative considerations. In the undoped case, the d^4 ion has $2S + 1$ sublevels with different spin projections M_S. The addition of a hole (electron) leads to filling of d^3 (d^5) terms with spins $S = 3/2$ ($S = 5/2$) and their spin projections M_S'. Since the electron spin is 1/2, projections M_S and M_S' must differ by 1/2. Nonzero matrix elements $\gamma_{\lambda\sigma}(m)$ in the case of annihilation of an electron exist for the following quasiparticles:

$$|d^4, M_S = +2\rangle + |\!\downarrow\rangle \;=\; \left|d^3, M'_S = +\frac{3}{2}\right\rangle,$$

$$|d^4, M_S = +1\rangle + |\!\downarrow\rangle \;=\; \left|d^3, M'_S = +\frac{1}{2}\right\rangle,$$

$$(15)$$

$$|d^4, M_S = 0\rangle + |\!\downarrow\rangle \;=\; \left|d^3, M'_S = -\frac{1}{2}\right\rangle,$$

$$|d^4, M_S = -1\rangle + |\!\downarrow\rangle \;=\; \left|d^3, M'_S = -\frac{3}{2}\right\rangle,$$

i.e., only four transitions take place. Analogously, we can easily write possible quasiparticles with spin up. The spectral weight and energy of quasiparticles depend on the type of magnetic state. In the FM phase, owing to splitting of local sublevels with different values of M_S in the internal field, only one state with $M_S = +S$ is filled and only one quasiparticle corresponding to the first relation in (15) has a nonzero spectral weight and dispersion. The remaining transitions between empty sublevels are characterized by a certain energy $\Omega(M_S, M'_S) = E(d^3, M'_S) - E(d^4, M_S)$ but have zero spectral weight. In the limits of such a spin block, in which the root vectors correspond only to different components of the same spin multiplet $\alpha_m = \{M_S, M'_S\}$, matrix (13) has the split form because effective transport (10) does not explicitly depend on the spin.

In the PM phase, the situation is different. All sublevels are degenerate and filled uniformly. For example, $\langle X^{M_S, M_S}\rangle = (1-x)/(2S+1)$ for terms $|d^4, M_S\rangle$. As a result, the values of

$$F(\{M_S, M'_S\}) \;=\; \langle X^{M_S, M_S}\rangle + \langle X^{M'_S, M'_S}\rangle$$

differ from zero and are the same for all excitations (15). Nevertheless, the split form of hopping matrix (10) in index m of the root vector within a spin block leads to the formation on only one "collective" quasiparticle, which is the superposition of all processes (15) (see Fig. 1), instead of $2S + 1$ quasiparticles with close dispersions and spectral intensities. Indeed, all matrix elements $\gamma_{\lambda\sigma}(m)$ appearing in $\hat{T}_{\text{eff}}$ are constructed with combinations of the Clebsch–Gordan coefficients and can be written in the form

$$\gamma_{\lambda,\sigma}(m) \;=\; \gamma_\lambda(m) \begin{cases} u_1\!\left(M_{3/2} + \dfrac{1}{2}\right), & \sigma = \uparrow \\[2mm] v_1\!\left(M_{3/2} - \dfrac{1}{2}\right), & \sigma = \downarrow, \end{cases}$$

while the maximal amplitudes in the T_{pd} structure have the form

$$\gamma_{p_\alpha,\sigma}(\alpha_m) \approx \rho\, \delta\!\left(M_2, M_{3/2} + \sigma\right)$$

$$\times \beta_\mu(d_\lambda) B_\tau(p_\alpha, d_\lambda)$$

$$\times \begin{cases} u_1\!\left(M_{3/2} + \dfrac{1}{2}\right), & \sigma = \uparrow \\[2mm] v_1\!\left(M_{3/2} - \dfrac{1}{2}\right), & \sigma = \downarrow, \end{cases} \tag{16}$$

$$\gamma_{d_\lambda,\sigma}(m) \approx \delta\!\left(M_2, M_{3/2} + \dfrac{1}{2}\right)$$

$$\times \beta_\mu(d_{\lambda'}) B_\tau(d_\lambda, d_{\lambda'})$$

$$\times \begin{cases} u_1\!\left(M_{3/2} + \dfrac{1}{2}\right), & \sigma = \uparrow \\[2mm] v_1\!\left(M_{3/2} - \dfrac{1}{2}\right), & \sigma = \downarrow. \end{cases}$$

The contribution from one spin block to the dispersion is given by

$$\det\Bigg((E - \Omega_m)\hat{I} - 2\rho F(m)\sum_{\alpha\lambda} T_{p_\alpha d_\lambda}(\mathbf{k})$$

$$\times \Bigg[\sum_{\lambda'\lambda''} \beta_\mu(d_{\lambda'}) B_\tau(d_\lambda, d_{\lambda'})$$

$$\times \beta_\mu(d_{\lambda''}) B_\tau(p_\alpha, d_{\lambda''})\Bigg] (\hat{u}_{1\uparrow})^2 \Bigg) \;=\; 0,$$

$$(17)$$

$$\det\Bigg((E - \Omega_m)\hat{I} - 2\rho F(m)\sum_{\alpha\lambda} T_{p_\alpha d_\lambda}(\mathbf{k})$$

$$\times \Bigg[\sum_{\lambda'\lambda''} \beta_\mu(d_{\lambda'}) B_\tau(d_\lambda, d_{\lambda'})$$

$$\times \beta_\mu(d_{\lambda''}) B_\tau(p_\lambda, d_{\lambda''})\Bigg] (\hat{v}_{1\downarrow})^2 \Bigg) \;=\; 0,$$

where $\hat{I}$ is the unit matrix, and the row matrices $\hat{u}_{1\sigma}$ and $\hat{v}_{1\sigma}$ are formed by the elements

$$u_{1\sigma}(m = M_2 \longleftrightarrow M_{3/2})$$
$$= \delta(M_2, M_{3/2} + \sigma) u_1(M_{3/2} + \sigma), \tag{18}$$

$$v_{1\sigma}(m = M_2 \longleftrightarrow M_{3/2})$$
$$= \delta(M_2, M_{3/2} + \sigma) v_1(M_{3/2} + \sigma). \tag{19}$$

Here, the coefficients are given by

$$u_1^2(M_S) = \frac{S + M_S}{2S}, \quad v_1^2(M_S) = \frac{S - M_S}{2S},$$

$$\rho = \left.\frac{2S + 1}{2S}\right|_{S=2},$$

Table 1

m'	$\frac{3}{2} \longleftrightarrow 2$	$\frac{1}{2} \longleftrightarrow 1$	$-\frac{1}{2} \longleftrightarrow 0$	$-\frac{3}{2} \longleftrightarrow -1$	$-\frac{5}{2} \longleftrightarrow -2$
$\frac{3}{2} \longleftrightarrow 2$	$u_1^2(2)$	$u_1(2)u_1(1)$	$u_1(2)u_1(0)$	$u_1(2)u_1(-1)$	0
$\frac{1}{2} \longleftrightarrow 1$	$u_1(1)u_1(2)$	$u_1^2(1)$	$u_1(1)u_1(0)$	$u_1(1)u_1(-1)$	0
$-\frac{1}{2} \longleftrightarrow 0$	$u_1(0)u_1(2)$	$u_1(0)u_1(1)$	$u_1^2(0)$	$u_1(0)u_1(-1)$	0
$-\frac{3}{2} \longleftrightarrow -1$	$u_1(-1)u_1(2)$	$u_1(-1)u_1(1)$	$u_1(-1)u_1(0)$	$u_1^2(-1)$	0
$-\frac{5}{2} \longleftrightarrow -2$	0	0	0	0	0

Table 2

m'	$\frac{5}{2} \longleftrightarrow 2$	$\frac{3}{2} \longleftrightarrow 1$	$\frac{1}{2} \longleftrightarrow 0$	$-\frac{1}{2} \longleftrightarrow -1$	$-\frac{3}{2} \longleftrightarrow -2$
$\frac{5}{2} \longleftrightarrow 2$	0	0	0	0	0
$\frac{3}{2} \longleftrightarrow 1$	0	$v_1^2(1)$	$v_1(1)v_1(0)$	$v_1(1)v_1(-1)$	$v_1(1)v_1(-2)$
$\frac{1}{2} \longleftrightarrow 0$	0	$v_1(0)v_1(1)$	$v_1^2(0)$	$v_1(0)v_1(-1)$	$v_1(0)v_1(-2)$
$-\frac{1}{2} \longleftrightarrow -1$	0	$v_1(-1)v_1(1)$	$v_1(-1)v_1(0)$	$v_1^2(-1)$	$v_1(-1)v_1(-2)$
$-\frac{3}{2} \longleftrightarrow -2$	0	$v_1(-2)v_1(1)$	$v_1(-2)v_1(0)$	$v_1(-2)v_1(-1)$	$v_1^2(-2)$

and their products $((\hat{g}_{1\sigma})^2 = \hat{g}_{1\sigma}^+\hat{g}_{1\sigma}$, $g_{1\sigma} = \hat{u}_{1\sigma}$, $\hat{v}_{1\sigma}$, are just the matrices formed by the produces of the Clebsch–Gordan coefficients (see Tables 1 and 2) in accordance with possible transitions between various components of multiplets. In this case, we have $2S + 1$ quasiparticles, from which only one exhibits dispersion:

$$E_m(\uparrow) = \Omega_m + F(m)\xi(\mathbf{k})[u_1^2(2) + u_1^2(1)$$
$$+ u_1^2(0) + u_1^2(-1)]$$

$$= \Omega_m + \xi(\mathbf{k})F(m)\sum_{M_s = -S}^{S} u_1^2(M_S),$$

$$E_m(\downarrow) = \Omega_m + F(m)\xi(\mathbf{k})[v_1^2(1) + v_1^2(0)$$
$$+ v_1^2(-1) + v_1^2(-2)] \qquad (20)$$

$$= \Omega_m + \xi(\mathbf{k})F(m)\sum_{M_s = -S}^{S} v_1^2(M_S);$$

$$\xi(\mathbf{k}) = \rho\sum_{\alpha\lambda} T_{p_\alpha d_\lambda}(\mathbf{k})$$

$$\times\left[\sum_{\lambda'\lambda''}\beta_\mu(d_{\lambda'})B_\tau(d_\lambda, d_{\lambda'})\beta_\mu(d_{\lambda''})B_\tau(p_\alpha, d_{\lambda''})\right].$$

Since the spectral intensity differs from zero for only two quasiparticles with dispersion, which differ only in the spin projection, and

$$\sum_{M_s = -S}^{S} u_1^2(M_S) = \sum_{M_s = -S}^{S} v_1^2(M_S) = S + \frac{1}{2},$$

we can observe only one quasiparticle doubly degenerate in spin in the PM phase. Each quasiparticle is characterized by its own root vector $\boldsymbol{\beta}(\mu)$ in the form of a

linear superposition of root vectors from two noninter-secting sets $\boldsymbol{\alpha}_{M_S}(\uparrow)$ or $\boldsymbol{\alpha}_{M_S}(\downarrow)$:

$$\boldsymbol{\beta}(\uparrow) = \frac{1}{u_1(S)} \sum_{M_S=-S}^{S} u_1(M_S)\boldsymbol{\alpha}_{M_S}(\uparrow)$$

$$= \sum_{M_S=-S}^{S} \cos\left(\frac{\phi_{M_S}}{2}\right)\boldsymbol{\alpha}_{M_S}(\uparrow),$$

$$\boldsymbol{\beta}(\downarrow) = \frac{1}{v_1(-S)} \sum_{M_S=-S}^{S} v_1(M_S)\boldsymbol{\alpha}_{M_S}(\downarrow) \quad (21)$$

$$= \sum_{M_S=-S}^{S} \sin\left(\frac{\phi_{M_S}}{2}\right)\boldsymbol{\alpha}_{M_S}(\downarrow).$$

Each root vector characterizes a certain quasiparticle, and the set of phases ϕ_{M_S} is determined by the spin on the d shell. Owing to the same amplitude $T_{\mathrm{eff},mn}^{pd}(\mathbf{k})$ with which initial quasiparticles $\boldsymbol{\alpha}_{M_S}$ are added, a single macroscopic state (21) is formed. Ultimately, each pair of spin multiplets from different sectors of the configuration space, which is bound by nonzero elements $T_{\mathrm{eff},mn}(\mathbf{k})$, generates in the PM phase only one quasiparticle, for which the phase difference (angle between the quantization axes at different sites) $\theta = \phi_{M_S}(R_i) - \phi_{M_S}(R_{i+h})$ in (21) is assumed to be zero; i.e., all local quantization axes remain parallel. Since the "magnetic factor" in expressions (20) is given by

$$F(\{M_S, M_S\}) \sum_{M_S=-S}^{S} u_1^2(M_S)$$

$$= \left(\frac{S+1/2}{2S+1}\right) = \frac{1}{2}, \quad (22)$$

narrowing of the valence band in such a state is twice as large as in the FM state, in which the analogous factor is $F(\{+S, +S\})u_1^2(+S) = 1$. To calculate the electronic structure in the PM phase, like in the double exchange model, we introduce the angle between the quantization axes at neighboring sites: $\theta = \phi_{M_S}(R_i) - \phi_{M_S}(R_{i+h}) = \pi/2$. In this case, the magnetic factor of contraction of the band width in the PM phase changes to

$$F_{PM}(M_S) \sum_{M_S=-S}^{S} \cos\left(\frac{\phi_{M_S}+\theta/2}{2}\right)$$

$$\times \cos\left(\frac{\phi_{M_S}-\theta/2}{2}\right) = \frac{1}{2}\cos\frac{\theta}{2} \approx 0.35. \quad (23)$$

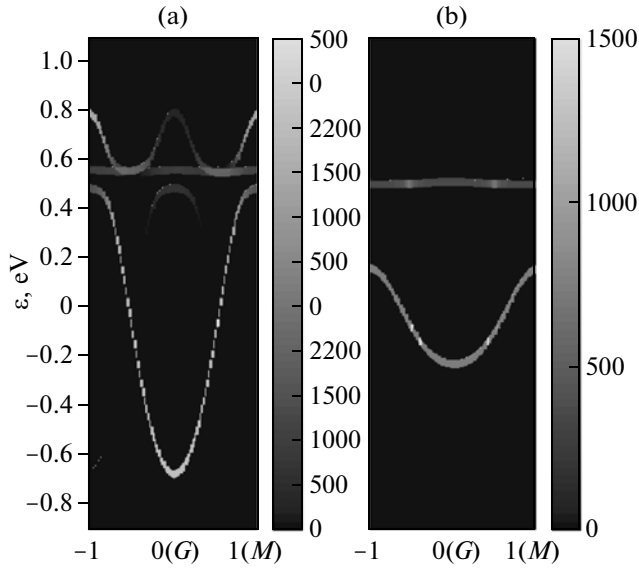Indeed, a stronger paramagnetic narrowing as compared to the DE model was also observed in [19], in which this factor is known to be $\cos(\theta/2)$. In the FM phase, in which only the basic component of the multiplet with spin in magnetization $F(\{+S, +S\}) = 1$ is occupied, a quasiparticle corresponding to only the given allowed transition with amplitude $T_{\mathrm{eff},mn}^{pd}(\mathbf{k}, \sigma)$ and angle $\phi_{M_S} = 0$ is observed. The quasiparticle with the opposite spin projection $\bar{\sigma}$ has zero spectral weight, and its contribution is zero at the Fermi level for $T = 0$; i.e., the ground state of the material is SHM with complete polarization at the Fermi level. Thus, upon the FP–PM transition at the Curie temperature, the type of the quasiparticle in the valence band changes; the quasiparticle in the SHM state, which exists only for $\phi_{M_S} = 0$, in the PM state is superposition (21) of quasiparticles, each of which is characterized by its own angle ϕ_{M_S} between the direction of spin S at the magnetic ion and the local quantization axis. The change in the nature of the quasiparticle is accompanied by narrowing of the band by factor (23).

4. NUMERICAL RESULTS

Following the previous qualitative analysis, we consider the results of numerical calculation of the spectral intensity of quasiparticle states in the PM and FM phases and draw conclusions concerning the possibility of the metal−insulator transition. We calculated the concentration points $x = 0.1-0.4$ with a step of $\Delta x = 0.05$. However, we will consider only the data for $x = 0.3$ because the results obtained for such values of parameters exhibit no singularities in concentration.

Figure 3 illustrates the relation between inter- and intrasublattice interactions; we calculated the spectral intensity along the symmetric [110] direction of the Brillouin zone ($x = 0.3$) in the FM and PM phases. We can observe the orbital ordering ($\sqrt{2} \times \sqrt{2}$) effects in the form of an additional superstructure in the spectral intensity of quasiparticle states. Figure 4 also show the corresponding dispersions of quasiparticle states, irrespective of their spectral intensity along symmetric directions in the cubic Brillouin zone.

In the FM phase, the ground SHM state is reproduced (see Fig. 4b), in which there is a band for a quasiparticle with the spin in magnetization, while the spectral intensity for a quasiparticle with the opposite spin projection is zero [36]. In the FM phase, the Fermi level lies in the valence band ($x \neq 0$), which is predominantly of the $d_{3y}(d_{3x})$ symmetry type and overlaps with the band of in-gap states of the Jahn−Teller origin with $d_x(d_y)$ symmetry (the classification is given in accordance with the contributions to spectral intensity (14) from particles with different orbital angular momenta). Due to this overlapping, the number $N_v(x)$ of quasiparticle states in the valence band exceeds the number of particles $N(x) = 7 - x$ per unit cell (one e_g

Fig. 3. Spectral intensity of quasiparticles in the valence band and in the band of in-gap states for (a) ferromagnetic and (b) paramagnetic phases for $x = 0.3$ along the [110] direction of the Brillouin zone. The right scale shows spectral intensity $A(\mathbf{k}, E)$ for the given energy and wavevector.

electron and six p electrons at three oxygen ions), and the Fermi level is in the valence band.

The dispersions and spectral intensities of bulk manganites were investigated in ARPES experiments [37, 38]. According to the results of observations, strong broadening of quasiparticle peaks takes place in the ARPES spectra. This effect is completely absent in our calculations because we disregarded the effects of orbital disorder, nonuniform charge distribution, etc., which lead to the decay of quasiparticle states. The calculated k dependences of the spectral intensity along the [110] symmetric direction in Fig. 4a in the FM phase reproduce the observed ARPES dependences only qualitatively (at least, for [38]).

Upon the transition to the PM phase, the SHM state disappears and the degeneracy in the quasiparticle spin projection is restored. Along with paramagnetic narrowing of the valence band, the nature of the quasiparticle itself changes. Analogous analysis with the introduction of local quantization axes can also be carried out for cuprates [39]. We have also found that the band narrowing effect removes overlapping of the valence band and the band of in-gap states in the PM phase.
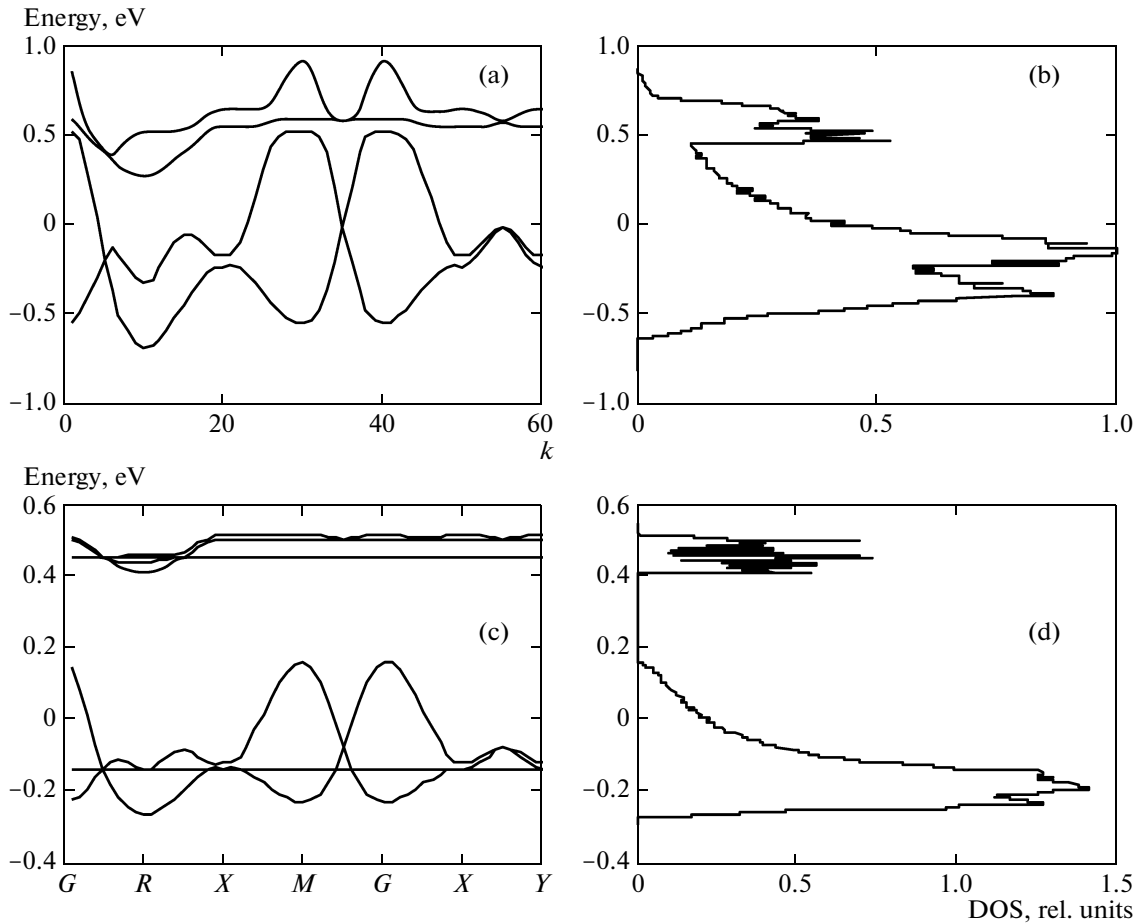
In contrast to calculations of the spectral intensity, subsequent calculations of the position of the Fermi level are much more complicated even in the zero-loop Hubbard I approximation. The origin of these problems is clarified in Fig. 1. The position of the Fermi level in complex systems with SECs cannot be analyzed by calculating the number of valence states only in the upper valence band (transitions 1 in Fig. 1). As a matter of fact, in the sum rule [41], all states

appear with a number of holes $N_h = 0, 1, 2, 3$ of the configuration space. Any constraint on the configuration space imposed after the procedure of diagonalization of H_0 violates the sum rule. Even in our incomplete pd formulation of the problem, we have

$$N = \int_{-\infty}^{E_F} dE \sum_\sigma \int d^3k \{A_\sigma(\mathbf{k}, E)\} = \int_{-\infty}^{E_F} dE$$

$$\times \int d^3k \left(-\frac{1}{\pi}\right) \sum_\sigma \sum_\nu \mathrm{Im}\{G_\sigma^{\nu\nu}(\mathbf{k}, E)\}_{E+i0}$$

$$= \int_{-\infty}^{E_F} dE \sum_\sigma \sum_{mn} \gamma_{\nu\sigma}(m)\gamma_{\nu\sigma}(n) \tag{24}$$

$$\times \left(-\frac{1}{\pi}\right) \int d^3k \, \mathrm{Im}\{D^{mn}(\mathbf{k}, E)\}_{E+i0},$$

where quasiparticles with transitions to all states in the two-hole sector are sorted in the sum over m and n ($\sim 10C_5^2$ is the approximate number of distributions of two holes over five states: two states e_g and three p states taking into account the total multiplicity of spin configurations: $S = 5/2$ and $S = 3/2$, which give a nonzero contribution to (24)), which form the packet of valence bands. Taking into account spin degeneracy $(2S + 1) = 5$ of the ground state in the one-particle spectrum in the PM phase, the dimensionality of matrix Green's function (11) for the two sublattices is $10^3 \times 10^3$ ($T = 0$). To determine the position of the Fermi level, the latter dimensionality must be calculated from the 3D Brillouin zone (integral with respect to $\mathbf{k}$ in (24)). We can now easily evaluate the integral with respect to energy variable E. On the $N^3 = 10^6$-point $\mathbf{k}$ basis, the total number of elements of the symmetric matrix is $(10^3)^2 \times 10^6/2 = 5 \times 10^{11}$ for calculation for one of the hole concentrations. In this case, our numerical algorithm for calculating Green function (11) leads to a long computer time in actual practice. Moreover, in the case of a nonzero temperature, we must also take into account all excited states in the one-particle spectrum in the sum over m and n.

Difficulties of fundamental nature also exist. In numerical identification of the dielectric state, exact answer cannot be obtained even for $T = 0$: the Fermi level with computer accuracy always lies in the band; i.e., we have a metal or a "poor" metal if the density of states at the Fermi level is low. Since it is impossible to reduce our configuration space due to excited states, we propose that all of them be taken into account, but in calculating the capacity of the packet of valence band, we must perform analytic calculations by formula (24) in the zeroth approximation in the effective hopping connecting different cells. Following this ideology, we will not be able to determine the specific position of the Fermi level in any band because dispersion is zero. However, we can nevertheless determine

Fig. 4. Dispersion, density of states, and Fermi level for $x = 0.3$ for the spin directed along the magnetization in the FM phase (a, b) and with spin degeneracy in the PM phase (c, d). The density of states in the SHM state with spin down is low (on the order of 10^{-8}) as compared to that with spin up at $T = 0$.

whether the Fermi level is in the band or in the dielectric gap. The total number of valence states is

$$N_v(x) = N_v^{12}(x) + N_v^{23}(x) = 7 - \left[1 - \frac{N_{frs}}{2}\right]x \approx 7$$

(see (A.9)); here, N_{frs} is the number of states of holes with the minimal energy in the band (first removal states, frs [40]). In our case, this is the quasiparticle depicted in Fig. 1 by the curve with number 1. Since the number of electrons per formula unit is $N = 7 - x$, the Fermi level falls to the band of valence states, and we can state that for the homogeneous PM state for $x \neq 0$ is of the metal type. To calculate the position of the Fermi level, we calculate the number of valence states in all valence bands, excluding the frs band:

$$\Delta N_v = N_v(x) - N_{frs} = 7 - \left[1 - \frac{N_{frs}}{2}\right]x - \frac{N_{frs}}{2}$$
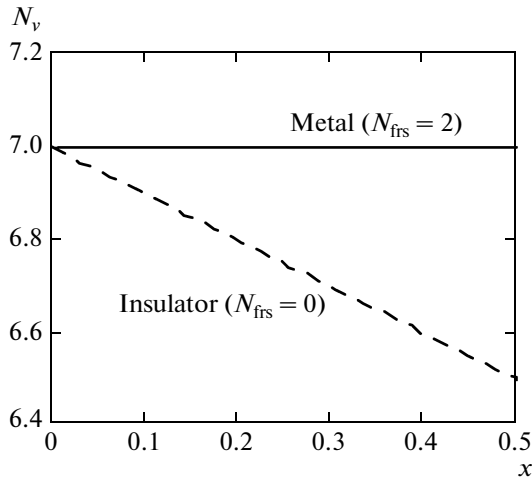$$= 7 - x - \frac{(1-x)N_{frs}}{2}. \tag{25}$$

The following effect, which is unusual for the simple Hubbard model, is observed. In undoped SEC materi-

als with a number of orbital states per cell exceeding two, the total number of states in the band with an arbitrary root vector m is not necessarily equal to a positive integer (see (A.7)). For parameters (3) obtained from LDA calculations, the number of states in the frs band calculated by formula (A.8) is $N_{frs} \approx 2$. The total number of electrons is distributed over the frs band and deeper lying states in the packet of valence bands (their number is ΔN_v). The number of electrons remaining in the frs band is

$$\Delta N = N - \Delta N_v \approx \frac{(1-x)N_{frs}}{2} \approx 1 - x. \tag{26}$$

Figures 4b and 4d shows the positions of the Fermi level calculated by this formula in the Hubbard I approximation under the conditions of reduction of configuration space for various doping levels in the PM and FM phases. As expected, this took a much shorted computer time, and the ground state for parameters (3) was found to be of the metal type.

It should be noted that the activation type of conductivity with a quadratic dependence of the activa-

Fig. 5. Dependence of number $N_v(x)$ of valence states on the doping level of the material under prohibition in selection rules (A.13) imposed on frs states (dashed line) at the top of the valence band and of allowed states (A.11) (solid line). Number of particle per cell is $N(x) = 7 - x$.

tion energy on the magnetization is considered in [21] as the universal reason for the metal−insulator transition (MIT) and colossal magnetoresistance (CMR) effects. Such a scenario takes place only if objective reasons exist for the Fermi level location in the gap for various concentrations. In the case of a homogeneous ground state, this can be compounds with forbidden frs states (see Appendix). Indeed, the effects of filling of the valence band in manganites are possible in principle irrespective of the doping level (see Fig. 5) if the exclusion for frs quasiparticles operates ($N_{frs} \approx 0$).

Since $\beta_0^2(d_x) \approx 1$ is an undoped material (see Fig. 2a), the dielectrization effects in manganites must be accompanied with filling of d_x orbitals upon an increase in doping level x. Such effects are not observed in the simple Hubbard model because the selection rules are identically obeyed in the calculation of matrix elements (A.4) of one-electron operators and do not prohibit any Fermi quasiparticles.

Another unobvious consequence of calculations (A.9) is worth mentioning: The material remains generally dielectric irrespective of the degree of degeneracy of the ground state in the unit cell of an undoped material with strong correlations. This conclusion is completely opposite to the results of calculations [1] based on the LDA method, in which the electron spectrum of LaMnO$_3$ manganites becomes metallic in the absence of Jahn−Teller distortions.

5. CONCLUSIONS

Thus, analysis of homogeneous FM and PM states based on the LDA + GTB method taking into account orbital ordering and SEC effects in the Hubbard I approximation leads to the SHM ground state with complete spin polarization. The PM phase is characterized by the narrowing of the band by a factor of (23) and by the superposition-type quasiparticles (22). The band structure calculated for the homogeneous FM and PM phases using the LDA parameters demonstrates the metallic behavior. The conditions under which the Fermi level in the PM phase can still be in the gap of the Jahn−Teller origin are determined. Indeed, the paramagnetic narrowing of the valence band (23) turns out to be stronger than the splitting of the in-gap band in it due to the Jahn−Teller effect; it is possible to observe the effects of filling only in the PM phase in materials with forbidden frs states.

APPENDIX

In the zeroth approximation for $A_\sigma(\mathbf{k}, E)$, the idea of calculating the position of the Fermi level can be implemented for an arbitrary number of orbitals per unit cell proceeding from the similarity between the set of all possible combinations $\beta_\mu(h_\lambda) B_\tau(h_\lambda', h_{\lambda''})$ and amplitudes $\gamma_{v\sigma}(\alpha_m) = \langle p | (\hat{c}^+_{v f\sigma}) | q \rangle$, where $|p\rangle$ is the state in the one-particle sector

$$|1h_{\mu, M_2}\rangle = \sum_\lambda \beta_\mu(h_\lambda) |h_\lambda, M_2\rangle$$

and $|q\rangle$ is one of all possible states

$$|2h_{\tau, M_S}\rangle = \sum_{\lambda\lambda'} B_\tau(h_\lambda, h_{\lambda'}) |h_\lambda, h_{\lambda'}, M_S\rangle.$$

Here, μ and τ denote the ground and excited states in the one- and two-particle sectors of the configuration space. In calculating the total number of valence states of quasiparticles, we must perform summation over all ground and excited states. In $\beta_\mu(h_\lambda)$ and $B_\tau(h_\lambda, h_{\lambda'})$, we will omit the spin dependence of states $|h_\lambda, M_2\rangle$ and $|h_\lambda, h_{\lambda'}, M_S\rangle$; i.e., the weights of the latter states are determined only by the distribution of holes (electrons) over the orbitals of a cell and not by the total spin on it. This will enable us to subsequently sum

matrix elements over μ, τ and spin indices S and M_S independently.

Let us introduce the concept of an additional particle in a state with orbital index ν (i.e., in the state on which the operator of the number of particles is acting in definition (24) of the spectral intensity). We single out this state from others because the participation of such a particle in the calculation of matrix elements with (24), it is important to sum correctly the spin moments of the additional particle and moment S of the remaining particles in our cell.

Calculation of the Clebsch–Gordan coefficients shows that the values of $\gamma_{\lambda\sigma}(\alpha_m)$ differ from pair products $\beta_\mu(h_\lambda)B_\tau(h_{\lambda'}, h_{\lambda''})$ in the phase determined by the spin nature of the corresponding states. Indeed, the function of the state with spin S' and spin projection M', which is expressed in terms of the states of an additional particle with spin σ and the state of the remaining particles with spin S in the cell in the two-hole sector with $N_h = 2$, has the form

$$|d_\lambda, d_{\lambda'}, M_{3/2}\rangle = |d^3, S = 3/2, M_{3/2}\rangle|0\rangle,$$

$$|d_\lambda, p_\alpha, M_{3/2}\rangle$$

$$= \sum_\sigma \Gamma_{2, \eta(\sigma)M}^{(S-|\sigma'|)}|d^4, S = 2, M_2 + \bar{\sigma}\rangle|p_{\alpha\sigma}\rangle. \quad (A.1)$$

These states are supplemented with a high-spin partner

$$|d_\lambda, p_\alpha, M_{5/2}\rangle$$

$$= \sum_\sigma \Gamma_{2, \eta(\sigma)M}^{(S+|\sigma'|)}|d^4, S = 2, M_2 + \bar{\sigma}\rangle|p_{\alpha\sigma}\rangle. \quad (A.2)$$

The contributions to $|2h_{\tau M_S}\rangle$ from the configurations with two holes on p orbitals of oxygen $|p_\alpha, p_{\alpha'}, M_{S=3/2+7/2}\rangle$ are calculated analogously. State $|d_\lambda, d_{\lambda'}, M_{3/2}\rangle$ has no partner because it is assumed that rigid spin $S = 3/2$ exists in the $(t_{2g})^3$ shell. In the one-hole sector with $N_h = 1$, the ground state with spin $S = 2$ has the form

$$|d_\lambda, M_2\rangle = |d^4, M_2\rangle$$

$$= \sum_\sigma \Gamma_{1, \eta(\sigma)M}^{(S+|\sigma|)}|d^3, S = 3/2, M_{3/2} + \bar{\sigma}\rangle|d_{\lambda\sigma}\rangle,$$

$$|p_\alpha, M_2\rangle \quad (A.3)$$

$$= \sum_\sigma \Gamma_{1, \eta(\sigma)M}^{(S-|\sigma|)}|d^5, S = 5/2, M_{5/2} + \bar{\sigma}\rangle|p_{\alpha\sigma}\rangle,$$

where notation $\Gamma_{N_h, \eta(\sigma)M}^S$ (Clebsch–Gordan coefficients in sectors with $N_h = 1, 2$) is used for the coeffi-

cients of vector summation. Summation over the spin multiplet components gives

$$\sum_{M=-S}^{S} [\Gamma_{N_h, \eta(\sigma)M}^S]^2 = \frac{1}{2} + S$$

(see relations (20) and [42]). The general form of the matrix element is

$$\gamma_{\nu\sigma}(\alpha_m) = \sum_\lambda \sum_{\sigma'} \Gamma_{1, \eta(\sigma')M_S}^S$$

$$\times \sum_{\lambda', \lambda''} \sum_{\sigma''} \Gamma_{2, \eta(\sigma'')M_{S'}}^{S'} \langle h_\lambda, M_S|c_{\nu\sigma}^+|h_{\lambda'}, h_{\lambda''}, M_{S'}\rangle \quad (A.4)$$

$$\times \beta_\mu(h_\lambda)B_\tau(h_{\lambda'}, h_{\lambda''}).$$

Matrix elements differ from zero for $S' = S \pm |\sigma|$ (spin selection rule; e.g.,

$$\langle p_\lambda, M_2|p_{\nu\sigma}^+|p_{\lambda'}, p_{\lambda''}, M_{S' = S \pm |\sigma|}\rangle$$

$$= \langle d_\lambda, M_2|p_{\nu\sigma}^+|d_{\lambda'}, p_{\lambda''}, M_{S' = S \pm |\sigma|}\rangle = 0$$

for $S' = 7/2$), as well as for $\nu = \lambda'$, $\lambda = \lambda''$ (orbit selection rule; the values of λ' and λ'' may coincide). For a number of particles smaller than or equal to two at a site, the spin selection rule holds, while for the number of orbitals smaller than or equal to two, the orbit selection rule operates (these are identities of permissive type). Calculating the position of the Fermi level in the zeroth approximation ($T = 0$), we obtain

$$N \approx \int_{-\infty}^{E_F} dE \sum_{\nu\sigma} \sum_{mn} \gamma_{\nu\sigma}(m)\gamma_{\nu\sigma}(n)\left(-\frac{1}{\pi}\right)$$

$$\times \mathrm{Im}\,\delta_{mn}D_{mn}^{(0)}(E)_{E+i0}$$

$$= \sum_{\nu\sigma}\left\{ \sum_{M=-S}^{S} F_{\mu=0}(x)\sum_\lambda \Gamma_{1, \eta(\sigma)M}^S \beta_{\mu=0}(h_\lambda) \quad (A.5)\right.$$

$$\times \sum_\tau \sum_{\sigma'=-1/2}^{+1/2} \Gamma_{2, \eta(\sigma)M'}^{(S+\sigma')} B_\tau(h_\lambda, h_\nu)$$

$$\left. \times \delta(M, M + \bar{\sigma}) \right\}^2,$$

where we have used summation over τ and over spin partners $S' = S \pm |\sigma|$ instead of the sum over root vectors α_m. The ground state in the one-hole sector of manganites is a high-spin state ($S = 2$) with predominant contribution $\beta_0(d_x)^2 = 1$ (Fig. 2a). All $2S + 1$ components of the spin multiplet are populated; i.e.,

$$F_{\mu=0}(x) = \delta_{\mu, 0}\delta_{S, 2}\frac{1-x}{2S+1}.$$

Let us decompose the spectral intensity into two terms:

$$N = \sum_\sigma \sum_{M=-S}^{S} F_0(x)$$

$$\times \sum_\nu \left\{ \sum_\lambda \beta_0^2(h_\lambda) \sum_\tau B_\tau^2(h_\lambda, h_\nu) \right. \tag{A.6}$$

$$\left. + \sum_\tau O_{\nu\sigma}(\alpha_{0\tau}) \right\}.$$

The first term is independent of the sign of contributions $\beta_0(h_\lambda)$ and $B_\tau(h_{\lambda'}, h_{\lambda''})$ from various orbital configurations, while the second is the sum of $O_{\nu\sigma}(\alpha_{0\tau})$ of all cross contributions with corresponding orbital and spin phases. In calculating the first term in (A.5), we have used

(i) completeness condition $\sum_\sigma [\Gamma_{N_h, \eta(\sigma)M}^{S'}]^2 = 1$ for the contributions from various spin states ($\sigma = \pm 1/2$) of the additional particle to the state with a fixed spin $S' = S \pm |\sigma'|$; for example, for the term with spin S in the two-hole sector, the contribution comes from a particle with spin $\sigma = 1/2$ and weight $[\Gamma_{2, \eta(\sigma)M}^{S'}]^2 = (S + M + 1/2)/(2S + 1)$ as well from a particle with spin $\sigma = -1/2$ and weight $[\Gamma_{2, \eta(\sigma)M}^{S'}]^2 = (S - M + 1/2)/(2S + 1)$;

(ii) completeness condition for the contributions from identical spin states of the additional particle to the states of different spin partners:

$$\sum_{S'=S-1/2}^{S'=S+1/2} [\Gamma_{N_h, \eta(\sigma)M}^{S'}]^2 = \sum_{\sigma'=-1/2}^{\sigma'=+1/2} [\Gamma_{N_h, \eta(\sigma)M}^{(S+\sigma')}]^2 = 1.$$

For example, an additional particle with spin $\sigma = \uparrow$ makes contributions to the high-spin state with weight $[\Gamma_{2, \eta(\sigma)M}^{S'=5/2}] = (S + M + 1/2)/(2S + 1)$, as well as to the low-spin state with weight $[\Gamma_{2, \eta(\sigma)M}^{S'=3/2}]^2 = (S - M + 1/2)/(2S + 1)$ of the two-hole sector. Consequently,

$$\frac{1}{2S+1} \sum_{M=-S}^{S} [\Gamma_{1, \eta(\sigma)M}^{S}]^2 \sum_{\sigma'=-1/2}^{+1/2} [\Gamma_{2, \eta(\sigma)M'}^{(S+\sigma')}]^2 = \frac{1}{2}.$$

The second term in formula (A.6) depends on the sign of the relevant coefficients (both orbital $\beta_0(h_\lambda)$ and $B_\tau(h_{\lambda'}, h_{\lambda''})$ and spin $\Gamma_{N_h, \eta(\sigma)M}^{S}$):

$$\sum_\tau O_{\nu\sigma}(\alpha_{0,\tau}) = \sum_\tau \Gamma_{1, \eta(\sigma)M}^{S} \sum_{\sigma'=-1/2}^{+1/2} \Gamma_{2, \eta(\sigma)M}^{(S+\sigma')}$$

$$\times \sum_{\lambda \neq \lambda'} \sum_{\nu \neq \lambda, \lambda'} [\beta_0(h_\lambda) B_\tau(h_\lambda, h_\nu)]$$

$$\times [\beta_0(h_{\lambda'}) B_\tau(h_{\lambda'}, h_\nu)] = 0,$$

because the sum

$$\sum_\tau [\beta_0(h_\lambda) B_\tau(h_\lambda, h_\nu)][\beta_0(h_{\lambda'}) B_\tau(h_{\lambda'}, h_\nu)] \approx 0$$

for any $\lambda \neq \lambda'$ and $\nu \neq \lambda, \lambda'$; i.e., the contribution from $O_{\nu\sigma}(\alpha_{0,\tau})$ to the total number of valence state is zero. Thus, for quasiparticles associated only with transitions from the ground state of the one-hole sector to the τ state of the two-hole sector, we obtain

$$N_{\tau, \sigma}^{12} = \frac{1}{2} \left\{ 1 + \beta_0^2(d_x) \right.$$

$$\left. \times \left[\sum_\alpha B_\tau^2(d_x p_\alpha) - \sum_{\lambda, \lambda' \neq d_x} B_\tau^2(h_\lambda h_{\lambda'}) \right] \right\}. \tag{A.7}$$

Here, $\tau = 0$, which corresponds to an frs quasiparticle; we have also used the identity

$$\sum_\lambda \beta_\mu^2(h_\lambda) \sum_{\lambda', \lambda''} B_\tau^2(h_{\lambda'} h_{\lambda''}) \equiv 1$$

for any μ and τ. Let us denote the number of frs states in the upper valence band by

$$N_{frs} = \sum_\sigma N_{\tau=0, \sigma}^{12} = 1 + \beta_0^2(d_x)$$

$$\times \left[\sum_\alpha B_\tau^2(d_x p_\alpha) - \sum_{\lambda, \lambda' \neq d_x} B_\tau^2(h_\lambda h_{\lambda'}) \right], \tag{A.8}$$

where $0 \leq N_{frs} \leq 2$. Summing expression (A.7) over all τ quasiparticle states in the two-hole sector, we find that the number of valence states in undoped manganite,

$$N_v = \sum_{\tau\sigma} N_\sigma^{12, j} = 10 + \beta_0^2(d_x)$$

$$\times \sum_{\tau=0}^{9} \left[\sum_\sigma B_\tau^2(d_x p_\alpha) - \sum_{\lambda, \lambda' \neq d_x} B_\tau^2(h_\lambda h_{\lambda'}) \right] \tag{A.9}$$

$$= 10 + (3 - 6) = 7$$

corresponds to the number of electrons per unit cell (i.e., we are dealing with an insulator). Let us determine the change in number $N_v(x)$ of the valence states with doping level x. The corresponding contribution to the number of valence states of quasiparticles associated with $1 \longleftrightarrow 2$ transitions is

$$N_v^{12}(x) = 7 - (7 - N_{frs}/2)x,$$

which is smaller than the number of particles $N(x) = 7 - x$ (see Fig. 5). We have disregarded the contribution from quasiparticle states associated with transi-

tions involving the states of a unit cell with three holes, $N_v^{23}(x)$ (see Fig. 1):

$$N_v^{23}(x) = \left\{ 1 + B_0^2(d_x, d_{3y}) \right.$$

$$\times \sum_{\eta=0}^{9} \left[\sum_\alpha D_\eta^2(d_x, d_{3y}, p_\alpha) \right. \tag{A.10}$$

$$\left. \left. - \sum_{\lambda, \lambda', \lambda''}{}' D_\eta^2(h_\lambda, h_{\lambda'}, h_{\lambda''}) \right] \right\} x$$

$$= (10 + (3-7))x = 6x,$$

since $B_0^2(d_x d_{3y}) \approx 0$ (see Figs. 2c). The prime on the sum over λ, λ', λ'' indicates that the terms of the type $D_\eta^2(d_x d_{3y} p_\mu)$ are not included, as well as $\beta_0(h_\lambda)$, $B_0(h_\lambda h_{\lambda'})$; here, $D_\eta(h_\lambda, h_{\lambda'}, h_{\lambda''})$ are the expansion coefficients of state $|3h_{\eta, M_s}\rangle$ ($\eta = 0$ to 9) over ten initial three-hole configurations in five orbitals. The total capacity of the packet of valence states,

$$N_v(x) = N_v^{12}(x) + N_v^{23}(x)$$

$$\approx 7 - \left[1 - \frac{N_{frs}}{2} \right] x \approx 7 \tag{A.11}$$

(see Fig. 5, metal), for other parameters (see (3)) of the Hamiltonian in the two-hole sector permits the existence of dielectrics for any doping level for $N_{frs} = 0$ with the forbidden frs state. For example, for a ground state with two holes in the oxygen shell or holes on the d_{3y} orbital and in the oxygen shell, $B_0^2(d_{3y}, p_\alpha) = 1$, we have

$$N_v(x) \approx 7 - \left[1 - \frac{N_{frs}}{2} \right] x \approx 7 - x, \tag{A.12}$$

where, in accordance with formula (A.8), we have

$$N_{frs} \approx 1 + \beta_0^2(d_x)$$

$$\times \left[\sum_\alpha B_0^2(d_x p_\alpha) - \sum_{\lambda, \lambda' \neq d_x} B_0^2(h_\lambda h_{\lambda'}) \right] \tag{A.13}$$

$$\approx 1 - \beta_0^2(d_x) \sum_\alpha B_0^2(d_{3y} p_\alpha) \approx 0,$$

which means that the total number of states in the valence band coincides with the number of particles $N(x)$ in the unit cell; i.e., dielectric materials are possible for any doping level. In any case, the dielectriza-

tion effects in manganites must be accompanied with filling of d_x (d_y) orbital with electrons; i.e.,

$$\sum_{\lambda \neq d_x} B_0^2(d_x h_\lambda) = 0$$

in the ground state of the two-hole sector.

REFERENCES

1. J. H. Pickett and D. Singh, Phys. Rev. B: Condens. Matter **53**, 1146 (1996).
2. J. H. Park, E. Vescovo, H.-J. Kim, C. Kwon, R. Ramesh, and T. Venkatesan, Nature (London) **392**, 794 (1998).
3. M. Bowen, M. Bibes, A. Barthelemy, J.-P. Contour, A. Anane, Y. Lemaitre, and A. Fert, Appl. Phys. Lett. **82**, 233 (2003).
4. M. Julliere, Phys. Lett. **69**, 363 (1996).
5. M. Imada, A. Fujimori, and Y. Tokura, Rev. Mod. Phys. **70**, 1039 (1998).
6. M. B. Salamon and M. Jaime, Rev. Mod. Phys. **73**, 583 (2001).
7. Yu. A. Izyumov and Yu. N. Skryabin, Usp. Fiz. Nauk **171** (2), 121 (2001) [Phys.—Usp. **44** (2), 109 (2001)].
8. M. Yu. Kagan and K. I. Kugel', Usp. Fiz. Nauk **171** (6), 577 (2001) [Phys.—Usp. **44** (6), 553 (2001)].
9. M. Yu. Kagan, A. V. Klaptsov, I. V. Brodskii, K. I. Kugel', A. O. Sboichakov, and A. L. Rakhmanov, Usp. Fiz. Nauk **173** (8), 877 (2003) [Phys.—Usp. **46** (8), 851 (2003)].
10. V. L. Aksenov, A. M. Balagurov, and V. Yu. Pomyakushin, Usp. Fiz. Nauk **173** (8), 883 (2003) [Phys.—Usp. **46** (8), 856 (2003)].
11. J. Coey, M. Viret, and S. von Molnar, Adv. Phys. **48**, 167 (1999).
12. M. Ziese, R. Höhne, N. Hong, J. Dienelt, K. Zimmer, and P. Esquinazi, J. Magn. Magn. Mater. **242–245**, 450 (2002).
13. A.-M. Haghiri-Gosnet and J.-P. Renard, J. Phys. D: Appl. Phys. **376**, R127 (2003).
14. K. Dorr, J. Phys. D: Appl. Phys. **39**, R125 (2006).
15. C. Zener, Phys. Rev. **82**, 403 (1951).
16. P. W. Anderson and H. Hasegawa, Phys. Rev. **100**, 675 (1955).
17. P. G. de Gennes, Phys. Rev. **118**, 141 (1960).
18. A. J. Millis, P. B. Littlewood, and B. I. Shraiman, Phys. Rev. Lett. **74**, 5144 (1995).
19. D. M. Edwards, A. C. Green, and K. Kubo, J. Phys.: Condens. Matter **11**, 2791 (1999); R. E. Brunton and D. M. Edwards, J. Phys.: Condens. Matter **10**, 5421 (1998).
20. A. J. Millis, Phys. Rev. B: Condens. Matter **53**, 8434 (1996); A. J. Millis, B. I. Shraiman, and R. Mueller, Phys. Rev. Lett. **77**, 175 (1996); A. J. Millis, R. Mueller, and B. I. Shraiman, Phys. Rev. B: Condens. Matter **54**, 5405 (1996).

21. N. G. Bebenin, R. I. Zainullina, V. V. Mashkautsan, V. V. Ustinov, and Ya. M. Mukovskii, Phys. Rev. B: Condens. Matter **69**, 104 434 (2004).

22. N. G. Bebenin, R. I. Zainullina, N. S. Bannikova, V. V. Ustinov, and Ya. M. Mukovskii, Phys. Rev. B: Condens. Matter **78**, 064 415 (2008).

23. N. G. Bebenin, N. N. Loshkareva, A. A. Makhnev, E. V. Mostovshchikova, L. V. Nomerovannaya, E. A. Gan'shina, A. N. Vinogradov, and Ya. M. Mukovskii, J. Phys.: Condens. Matter **22**, 096 003 (2010).

24. Y.-F. Yang and K. Held, Phys. Rev. B: Condens. Matter **76**, 212 401 (2007); K. Held and D. Vollhardt, Phys. Rev. Lett. **84**, 5168 (2000).

25. Adriana Moreo, Seiji Yunoki, and Elbio Dagotto, Phys. Rev. Lett. **83**, 2773 (1999).

26. H.-D. Chuang, A. D. Gromko, D. S. Dessau, T. Kimura, and Y. Tokura, Science (Washington) **292**, 1509 (2001).

27. J. O'Donnell, M. Onellion, M. S. Rzchovski, J. N. Eckstein, and I. Bozovic, Phys. Rev. B: Condens. Matter **54**, R6841 (1996).

28. V. A. Gavrichkov, S. G. Ovchinnikov, A. A. Borisov, and E. G. Goryachev, Zh. Eksp. Teor. Fiz. **118** (2), 422 (2000) [JETP **91** (2), 369 (2000)].

29. V. A. Gavrichkov, S. G. Ovchinnikov, and L. Yakimov, Zh. Eksp. Teor. Fiz. **129** (6), 1103 (2006) [JETP **99** (3), 559 (2004)].

30. M. M. Korshunov, V. A. Gavrichkov, S. G. Ovchinnikov, Z. V. Pchelkina, I. A. Nekrasov, M. A. Korotin, and V. I. Anisimov, Zh. Eksp. Teor. Fiz. **126** (3), 642 (2004) [JETP **99** (3), 559 (2004)].

31. K. I. Kugel' and D. I. Khomskii, Zh. Eksp. Teor. Fiz. **64** (4), 1429 (1973) [Sov. Phys. JETP **37** (4), 725 (1973)]; K. I. Kugel' and D. I. Khomskii, Usp. Fiz. Nauk **136** (4), 621 (1982) [Sov. Phys.—Usp. **25** (4), 231 (1982)].

32. A. J. Millis, in *Proceedings of the Summer College and Conference "Physics and Chemistry of Rare-Earth Manganites," Abdus Salam International Centre for Theoretical Physics (ICTP), Trieste, Italy, June 1–18, 2003* (Trieste, 2003), p. SMR1505/33.

33. V. Goldschmidt, *Geochemistry* (Oxford University Press, Oxford, 1958).

34. J. Hubbard, Proc. R. Soc. London, Ser. A **276**, 238 (1963).

35. Yu. A. Izyumov, Usp. Fiz. Nauk **165** (4), 403 (1995) [Phys.—Usp. **38** (4), 385 (1995)].

36. V. Yu. Irkhin and M. I. Katsnel'son, Usp. Fiz. Nauk **164** (7), 705 (1994) [Phys.—Usp. **37** (7), 659 (1994)].

37. M. Shi, M. C. Falub, P. R. Willmott, J. Krempasky, R. Herger, K. Hricovini, and L. Patthey, Phys. Rev. B: Condens. Matter **70**, 140 407 (2004).

38. M. C. Falub, M. Shi, P. R. Willmott, J. Krempasky, S. G. Chiuzbaian, K. Hricovini, and L. Patthey, Phys. Rev. B: Condens. Matter **72**, 054 444 (2005).

39. V. M. Loktev, Fiz. Nizk. Temp. (Kharkov) **31** (6), 645 (2003) [Low Temp. Phys. **31** (6), 490 (2003)].

40. A. Damascelli, Z. Hussain, and Z.-X. Shen, Rev. Mod. Phys. **75**, 473 (2003).

41. S. G. Ovchinnikov, Zh. Eksp. Teor. Fiz. **102** (2), 534 (1992) [Sov. Phys. JETP **75** (2), 283 (1992)].

42. R. O. Zaitsev, *Diagrammatic Methods in the Theory: Superconductivity and Ferromagnetism* (URSS, Moscow, 2004; URSS, Moscow, 2007).

Translated by N. Wadhwa